Hindawi Publishing Corporation
Journal of Chemistry
Volume 2015, Article ID 592951, 11 pages
http://dx.doi.org/10.1155/2015/592951

Research Article

Modeling Wettability Variation during Long-Term Water Flooding

Renyi Cao,[1] Changwei Sun,[1] and Y. Zee Ma[2]

[1]*School of Petroleum Engineering, China University of Petroleum, Beijing 102245, China*
[2]*Schlumberger, Denver, CO 80202, USA*

Correspondence should be addressed to Renyi Cao; caorenyi@gmail.com

Received 30 September 2014; Revised 20 January 2015; Accepted 18 March 2015

Academic Editor: Cengiz Soykan

Surface property of rock affects oil recovery during water flooding. Oil-wet polar substances adsorbed on the surface of the rock will gradually be desorbed during water flooding, and original reservoir wettability will change towards water-wet, and the change will reduce the residual oil saturation and improve the oil displacement efficiency. However there is a lack of an accurate description of wettability alternation model during long-term water flooding and it will lead to difficulties in history match and unreliable forecasts using reservoir simulators. This paper summarizes the mechanism of wettability variation and characterizes the adsorption of polar substance during long-term water flooding from injecting water or aquifer and relates the residual oil saturation and relative permeability to the polar substance adsorbed on clay and pore volumes of flooding water. A mathematical model is presented to simulate the long-term water flooding and the model is validated with experimental results. The simulation results of long-term water flooding are also discussed.

1. Introduction

Wettability is an important factor that affects oil recovery in water flooding. In the past, oil reservoirs were commonly interpreted to be strongly water-wet, because water phase is generally the initial fluid contact with the reservoir rock. However, some researchers found that many reservoir rocks were not strongly water-wet [1, 2]. The latter results were obtained without considering the natural surfactant in crude oil, such as asphalt and paraffin substances, which are easily absorbed on the solid-liquid interface and change reservoir rocks to oil-wet [3]. Kusakov [4] found that the rupture of water film could lead to crude oil directly contacting the quartz surface and the surface would become oil-wet instead of water-wet. Schmid [5] claimed that wettability could be changed and strong water-wet rock could become weak water-wet after contact with crude oil.

For the sandstone reservoirs, the wettability changes during deposition process, accumulation process, and water flooding process (Figure 1). During deposition process, the pores are saturated with water to form a layer of water film during the deposition process [6, 7], as shown in Figure 1(a). Thus, the reservoir rocks are water-wet. During the accumulation process, the partial polar substances in crude oil penetrate water film to adsorb on rock surface through van der Waals, electrostatic, hydrogen bonding, and acid-base [8–11], and the rock with the polar substances changes to oil-wet, as shown in Figure 1(b). Note, however, that if the partial polar substances do not penetrate water film, the rock will be water-wet. During long-term water flooding, the polar substances can be washed out and desorbed from the rock surface; the wettability may change to water-wet, as shown in Figure 1(c).

Wettability may affect almost all the variables in core analysis, including capillary pressure, relative permeability, oil recovery, and EOR. Morrow [12] confirmed that a higher water flooding recovery could be obtained in strongly water-wet core through one-dimensional water flooding experiments. The one-dimensional displacement experiments with high pore volume (PV) of injected water [13] showed that the changes of wettability and pore structure during long-term water flooding reduced the critical capillary number

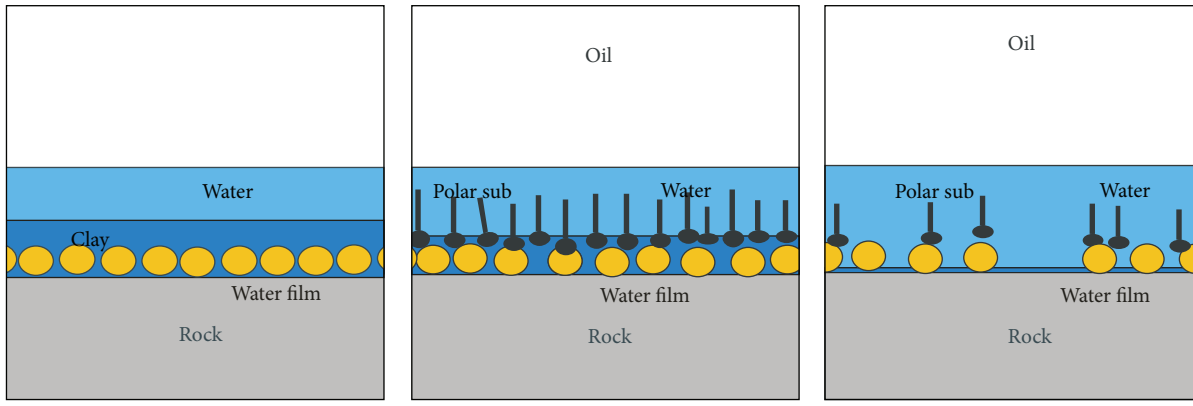

(a) Deposition process (b) Accumulation process (c) Water-flooding process

Figure 1: Wettability variation during reservoir formation process.

and the residual oil saturation. When the injected water was 5000 PV of rock core, the oil displacement efficiency of cores was about 57%; when the injected water was 1000 PV or even 10000 PV, the oil displacement efficiency was increased (near 80%) [13]. Therefore, under different water flooding conditions, oil displacement efficiency of the rock is not a constant.

The wettability changes during long-term water flooding, and this could affect the residual oil saturation and oil recovery. A number of studies showed that, during low-salinity water flooding, the ions could exchange between injecting water and rock, and it could lead to adsorption of divalent ions and minerals dissolution, change the wettability to water-wet, and enhance oil recovery [14–20]; it could also lead to changes of relative permeability [21–25]. Recently, mechanism on wettability alternation, such as surfactant flooding, gas displacement, and low salinity water flooding has been studied [16, 20, 26–30].

The main factor affecting wettability is the amount of polar substances adsorbed on the clay surface. In order to model the wettability variation, we should first evaluate the amount of polar substances adsorbed on the surface of clay. Five factors that impact the polar adsorption and desorption should be considered, and these include the concentration of polar substances in crude oil and on rock surface [31], salinity and pH of injecting water and formation water [32, 33], clay contents in rock [28], and flow rate of water through the pore [31]. Yet, an accurate description of wettability alternation model during long-term water flooding from injecting well or aquifer is lacking, which will lead to failure in history matching and unreliable forecasts using numerical simulation [34, 35].

The purpose of this paper includes: (1) characterizing the adsorption of polar substance during long-term water flooding from injecting water or aquifer and then relate the residual oil saturation and relative permeability to the polar substance adsorbed on clay and pore volumes of flooding water and (2) building a mathematical model to simulate the long-term water flooding. The simulation results of long-term water flooding are also discussed in this paper.

2. Mathematical Models for Long-Term Water Flooding

2.1. Conditions. The following conditions are assumed in our mathematical modeling for long-term water flooding.

(1) Temperature of reservoir is constant.

(2) Reservoir fluids are oil and water phases.

(3) Components include water, oil, polar substance (AO), clay, Na^+, Ca^{2+}, Mg^{2+}, Fe^{3+}, OH^-, and other anions.

(4) No phase transition process is in reservoir.

(5) Porosity and permeability don't change during long-term water flooding.

(6) Gravity is not considered.

2.2. Model of Variation for Polar Substances on the Rock Surface. The amount of polar substances adsorbed on the rock surface mainly is determined by the polar substances adsorbed on the clay and the content of clay in rock. The content of polar substances adsorbed on the rock can be described by

$$C_{\text{rock}}^{\text{AO}} = C_{\text{clay}}^{\text{AO}} \cdot C_{\text{rock}}^{\text{clay}}, \tag{1}$$

where $C_{\text{rock}}^{\text{AO}}$—concentration of polar substances (AO) adsorbed on the rock; $C_{\text{clay}}^{\text{AO}}$—concentration of polar substances (AO) adsorbed on the clay; and $C_{\text{rock}}^{\text{clay}}$—concentration of clay in the rock.

The clay could fall off from the rock surface by the water flushing under long-term water flooding, and this process can be described by

$$C_{\text{rock}}^{\text{clay}} \xrightarrow{\text{DESORPTION}} C_{\text{water}}^{\text{clay}}, \tag{2}$$

where $C_{\text{water}}^{\text{clay}}$—concentration of clay in the aqueous phase (water).

Assuming that the process for the clay desorption is nonlinear and the desorption rate is a function of the aqueous

phase flow rate v_w, the Langmuir adsorption law can be used to characterize it:

$$\frac{dC_{\text{rock}}^{\text{clay}}}{dt} = K_1 \cdot v_w \cdot \frac{c_{\text{rock}}^{\text{clay}}}{1 + bc_{\text{rock}}^{\text{clay}}}, \tag{3}$$

where $dC_{\text{rock}}^{\text{clay}}/dt$—desorption rate; K_1, b—clay desorption constant; and v_w—flow rate of water phase.

Equation (3) implies the influence of total volume of water flushing the rock surface during the long-term water flooding, because the rate of clay desorption in rock is related to the flow rate of water phase.

The equilibrium between the concentration of polar substances in the oil phase and the concentration of polar substances in clay mineral surface is expressed by

$$C_{\text{clay}}^{\text{AO}} \xleftrightarrow{\text{EQUILIBRIUM}} C_{\text{oil}}^{\text{AO}}, \tag{4}$$

where $C_{\text{oil}}^{\text{AO}}$—concentration of the polar substance (AO) in the oil phase.

This equilibrium can be represented by the exchange equilibrium equation with a coefficient, κ^{exm}, which is the equilibrium constant for the exchange between polar substances on the clay surface and the oil phase:

$$\kappa^{\text{exm}} = \frac{C_{\text{clay}}^{\text{AO}}}{C_{\text{oil}}^{\text{AO}}}. \tag{5}$$

Formation water salinity and pH influence adsorption of polar substances on the rock surface [18, 28]. The equilibrium constant κ^{exm} can be characterized as the relationship between the total concentration of the metal cations in formation water and the concentration of hydroxide ions:

$$\kappa^{\text{exm}} = K_2 \frac{\sum \left[\text{Na}^+\right]\left[\text{Ca}^{2+}\right]\left[\text{Mg}^{2+}\right]\left[\text{Fe}^{3+}\right]\cdots}{\left[\text{OH}^-\right]}, \tag{6}$$

where K_2—balance factor; $[\text{Na}^+][\text{Ca}^{2+}][\text{Mg}^{2+}][\text{Fe}^{3+}]$—the concentration of sodium ion in the aqueous phase.

2.3. Mass Conservation Equations and Pressure Equations. The continuity of mass for component k in association with Darcy's law is expressed as a function of the overall volume of component per unit pore volume ($\overline{C}_k$):

$$\begin{aligned}\frac{\partial}{\partial t}\left(\phi\overline{C}_k \cdot \rho_k\right) + \nabla\left[\sum_{l=1}^{n_p}\rho_k\left(C_{kl}\cdot\overline{U}_l - \widetilde{D}_{kl}\right)\right] \\ = Q_k + {Q_k}^T + {Q_k}^{FS} + {Q_k}^{TS},\end{aligned} \tag{7}$$

where n_{cv}—total number of volume-occupying components (including water, oil, and polar substances); n_p—number of phases; $\overline{C}_k$—adsorbed concentration of component k, $\overline{C}_k = 1 - [\sum_{k=1}^{n_{\text{cv}}}\widehat{C}_k]\sum_{l=1}^{n_p} S_l \times C_{kl} + \widehat{C}_k$, $k = 1, 2, \ldots, n_{\text{cv}}$; ρ_k—density of pure component k; Q_k—injection/output rate of component k with Unit volume; and ${Q_k}^T$—output rate of component k by reaction in phase l with unit volume. ${Q_k}^{FS}$ is output rate of component k solid-phase under mechanical force (long-term erosion) conditions with unit volume. For clay component, it can be determined by (3). ${Q_k}^{TS}$ is output rate of ion balance for component k on rock surface with unit volume.

The output rate of polar substances and clay components can be determined by

$${Q_k}^T = \sum_{l=1}^{n_p} S_l \cdot K_{kl}^{\text{exm}} C_{\text{rock}}^k, \tag{8}$$

$${Q_k}^{FS} = K_1 \cdot v_w \cdot \frac{c_{\text{rock}}^{\text{clay}}}{1 + bc_{\text{rock}}^{\text{clay}}}, \tag{9}$$

$${Q_k}^{TS} = K^{\text{exm}} C_{\text{rock}}^k, \tag{10}$$

where $K_{kl}^{\text{exm}} = dC_l^k/dt$ is the output rate of component k in the liquid phase l and K_1 is deposition rate of component k on the rock surface; consider

$$K^{\text{exm}} = k_2 \frac{\sum \left[\text{Na}^+\right]\left[\text{Ca}^{2+}\right]\left[\text{Mg}^{2+}\right]\left[\text{Fe}^{3+}\right]}{\left[\text{OH}^-\right]}. \tag{11}$$

The aqueous-phase pressure is obtained by an overall mass balance on volume components [36]. Because of the following condition

$$\sum_{k=1}^{n_{\text{cv}}} C_{kl} = 1, \tag{12}$$

the pressure equation in terms of the reference phase pressure (phase 1) is

$$\begin{aligned}&\phi C_t \cdot \frac{\partial p_1}{\partial t} + \nabla\overline{\overline{K}} \cdot \lambda_{rTc} \cdot \nabla p_1 \\ &\quad = -\nabla\sum_{l=1}^{n_p}\overline{\overline{K}} \cdot \lambda_{\text{rec}} \cdot \nabla h + \nabla \cdot \sum_{l=1}^{n_p}\overline{\overline{K}} \cdot \lambda_{rTc} \cdot \nabla p_{cl1} \\ &\qquad + \sum_{l=1}^{n_p}\left(Q_k + {Q_k}^T + {Q_k}^{FS} + {Q_k}^{TS}\right),\end{aligned} \tag{13}$$

where $\lambda_{\text{rec}} = (k_{rl}/\mu_l)\cdot\sum_{k=1}^{n_{\text{cv}}}\cdot\rho_k\cdot C_{kl}$; $\lambda_{rTc} = \sum_{l=1}^{n_p}\lambda_{\text{rec}}$ is the total relative mobility with the correction for fluid compressibility.

The total compressibility C_t is the volume-weighted sum of the rock or soil matrix (C_r) and component compressibilities (C_k^0) are

$$C_t = C_r + \sum_{k=1}^{n_{\text{cv}}} C_k^0 \cdot \widetilde{C}_k, \tag{14}$$

where $\phi = \phi_R \cdot [1 + C_r(p_{\text{ref}} - p_{\text{ref}_0})]$.

2.4. Relative Permeability Model. During long-term water flooding, the wettability changes with the reduction of polar substances on the rock surface, and the residual oil saturation and displacement oil efficiency will change as well. Since the

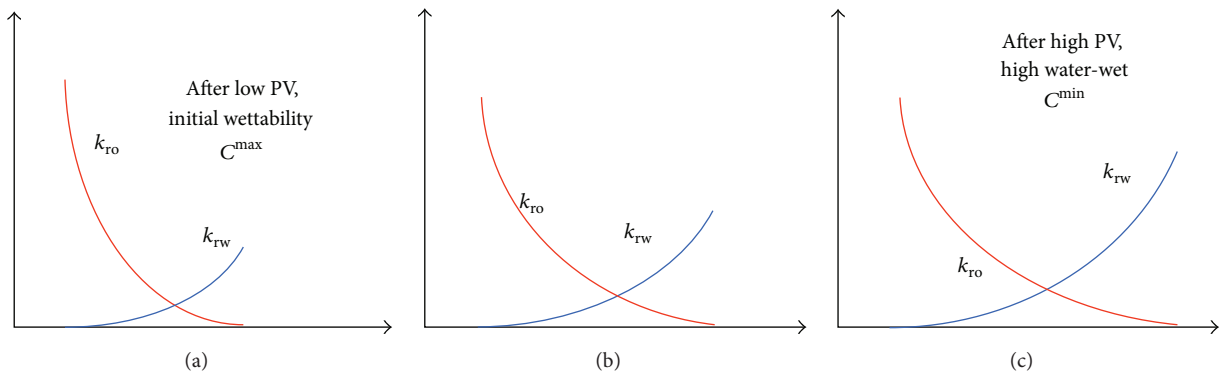

FIGURE 2: Relative permeabilities determined at different pore volumes of water injected.

polar substances on the rock surface is not constant, which depends on the time of displacement and flow rate of water phase, the residual oil saturation is a function of flow rate and time of water flooding (the cumulative volumes of water displacement).

Since the variation of wettability is reflected by the relative permeabilities and residual oil saturation, different relative permeabilities (which could be measured with cores after different volumes of water displacement, Figure 2) can be used to calculate the residual oil saturation and displacement oil efficiency [28].

The relative permeability curve at low PV (initial wettability, Figure 2(a)) of injected water reflects the initial wettability of rock with maximum contents ($C_{\text{rock}}^{\text{AO max}}$ represented by $C^{\max}$) of polar substances adsorbed on rock; the relative permeability curve at high PV (high water-wet at ultimate water displacement, Figure 2(c)) of injected water reflects the initial wettability of rock with minimum contents ($C^{\min}$) of polar substances adsorbed on rock. We can use $C_{\text{rock}}^{\text{clay}}$ to interpolate the relative permeabilities and residual oil saturation (Figure 2(b)) at different PV of injected water.

Given relative permeability curves at $C^{\max}$ and $C^{\min}$, we can determine the maximum and minimum residual oil saturation, and the residual oil saturation S_{or} can be calculated with the linear interpolation methods [27]:

$$S_{\text{or}} = S_{\text{or}}^{\max} - \frac{C - C^{\min}}{C^{\max} - C^{\min}} \left(S_{\text{or}}^{\max} - S_{\text{or}}^{\min}\right), \tag{15}$$

where $S_{\text{or}}^{\max}$—the residual oil saturation at $C^{\max}$ (low PV, initial wettability); $S_{\text{or}}^{\max}$—the residual oil saturation at $C^{\min}$ (high PV, high water-wet wettability).

The endpoints of relative permeabilities are computed with a linear interpolation between the given input values at $C^{\max}$ and $C^{\min}$,

$$K_{rl\text{end}} = K_{rl\text{end}}^{\max} - \frac{S_{\text{or}} - S_{\text{or}}^{\min}}{S_{\text{or}}^{\max} - S_{\text{or}}^{\min}} \left(K_{rl\text{end}}^{\max} - K_{rl\text{end}}^{\min}\right), \tag{16}$$

where $K_{rl\text{end}}$—the endpoint of relative permeability for phase l at S_{or}; $K_{rl\text{end}}^{\max}$—the endpoint of relative permeability for phase l at $S_{\text{or}}^{\max}$; and $K_{rl\text{end}}^{\min}$—the endpoint of relative permeability for phase l at $S_{\text{or}}^{\min}$.

The relative permeabilities for phase l are assumed to be unique functions of their respective saturations only [37], described as

$$K_{rl} = K_{rl\text{end}} \left(S_l^*\right)^n, \tag{17}$$

where S_l^*—the normalized saturations for phase l, $S_w^* = ((S_w - S_{wc})/(1 - S_{wc} - S_{\text{or}}))$, $S_o^* = 1 - S_w^*$; and n—the exponent determined by fitting the data.

3. Numerical Models

Based on (7), the polar substances and clay only dissolve in water phase, and the governing equations can be described as follows:

$$\begin{aligned}
&\frac{\partial\left(\varphi\lambda_k\rho_k\widetilde{C}_{k,w}\right)}{\partial t} \\
&\quad + \frac{\partial}{\partial x}\left[\rho_k\left(C_{k,w}u_{xw} - \varphi S_w\left(K_{xxkw}\frac{\partial C_{k,w}}{\partial x} + K_{xykw}\frac{\partial C_{k,w}}{\partial y} + K_{xzkw}\frac{\partial C_{k,w}}{\partial z}\right)\right)\right] \\
&\quad + \frac{\partial}{\partial y}\left[\rho_k\left(C_{k,w}u_{yw} - \varphi S_w\left(K_{yxkw}\frac{\partial C_{k,w}}{\partial x} + K_{yykw}\frac{\partial C_{k,w}}{\partial y} + K_{yzkw}\frac{\partial C_{k,w}}{\partial z}\right)\right)\right] \\
&\quad + \frac{\partial}{\partial z}\left[\rho_k\left(C_{k,w}u_{zw} - \varphi S_w\left(K_{zxkw}\frac{\partial C_{k,w}}{\partial x} + K_{zykw}\frac{\partial C_{k,w}}{\partial y} + K_{zzkw}\frac{\partial C_{k,w}}{\partial z}\right)\right)\right] \\
&\quad = R_k \quad k = 1, 2, \ldots, n_{\text{cv}},
\end{aligned} \tag{18}$$

where

$$\lambda_k = \left(1 - \sum_{m=1}^{n} \widehat{C}_m\right) S_w,$$

$$\begin{bmatrix} K_{xxkw}, & K_{xykw}, & K_{xzkw} \\ K_{yxkw}, & K_{yykw}, & K_{yzkw} \\ K_{zxkw}, & K_{zykw}, & K_{zzkw} \end{bmatrix}, \tag{19}$$

is the diffusion tensor of component k, $R_k = Q_k + Q_k^{\,T} + Q_k^{\,FS} + Q_k^{\,TS}$.

If the water phase is selected as the reference phase, with the assumption that the component of oil cannot be dissolved in water phase, the pressure equation in water phase is expressed as

$$\phi C_t \frac{\partial p_w}{\partial t} - \nabla\left(\overline{\overline{K}}\lambda_{rtc}\nabla p_w\right) = \sum_{k=1}^{n_{cv}} R_k. \tag{20}$$

The oil phase pressure equations can be computed by adding the capillary pressure between phases. The implicit form to process the pressure of water phase P_w and the explicit form to process the coefficients can be used:

$$\begin{aligned}
&(\varphi C_t V)^n \frac{\left(P_{w,i}^{n+1} - P_{w,i}^{n}\right)}{\Delta t} \\
&\quad - \Delta y \Delta z \left[\left(\overline{\overline{K}}\lambda_{rtc}\right)_{i+1/2}^{n} \frac{P_{w,i+1}^{n+1} - P_{w,i}^{n+1}}{\Delta x_{i+1/2}} - \left(\overline{\overline{K}}\lambda_{rtc}\right)_{i-1/2}^{n} \frac{P_{w,i}^{n+1} - P_{w,i-1}^{n+1}}{\Delta x_{i-1/2}}\right] \\
&\quad - \Delta x \Delta z \left[\left(\overline{\overline{K}}\lambda_{rtc}\right)_{j+1/2}^{n} \frac{P_{w,j+1}^{n+1} - P_{w,j}^{n+1}}{\Delta y_{j+1/2}} - \left(\overline{\overline{K}}\lambda_{rtc}\right)_{j-1/2}^{n} \frac{P_{w,j}^{n+1} - P_{w,j-1}^{n+1}}{\Delta y_{j-1/2}}\right] \\
&\quad - \Delta x \Delta y \left[\left(\overline{\overline{K}}\lambda_{rtc}\right)_{m+1/2}^{n} \frac{P_{w,m+1}^{n+1} - P_{w,m}^{n+1}}{\Delta z_{m+1/2}} - \left(\overline{\overline{K}}\lambda_{rtc}\right)_{m-1/2}^{n} \frac{P_{w,m}^{n+1} - P_{w,m-1}^{n+1}}{\Delta z_{m-1/2}}\right] \\
&\quad = V \sum_{k=1}^{Ncv} R_k.
\end{aligned} \tag{21}$$

Define

$$T_{l,i\pm1/2} = \frac{\Delta y \Delta z \left(\overline{\overline{K}}\lambda_{rlc}\right)_{i\pm1/2}^{n}}{\Delta x_{i\pm1/2}},$$

$$T_{l,j\pm1/2} = \frac{\Delta x \Delta z \left(\overline{\overline{K}}\lambda_{rlc}\right)_{j\pm1/2}^{n}}{\Delta y_{j\pm1/2}},$$

$$T_{l,m\pm1/2} = \frac{\Delta y \Delta z \left(\overline{\overline{K}}\lambda_{rlc}\right)_{m\pm1/2}^{n}}{\Delta z_{m\pm1/2}},$$

Table 1: Parameters of the numerical model.

Parameters	Values
Porosity	0.25
Permeability/mD	1000
Grid numbers	100
Length/cm	7.5

$$T_{tw,i\pm1/2} = \frac{\Delta y \Delta z \left(\overline{\overline{K}}\lambda_{rtc}\right)_{i\pm1/2}^{n}}{\Delta x_{i\pm1/2}},$$

$$T_{tw,j\pm1/2} = \frac{\Delta x \Delta z \left(\overline{\overline{K}}\lambda_{rtc}\right)_{j\pm1/2}^{n}}{\Delta y_{j\pm1/2}},$$

$$T_{tw,m\pm1/2} = \frac{\Delta y \Delta z \left(\overline{\overline{K}}\lambda_{rtc}\right)_{m\pm1/2}^{n}}{\Delta z_{m\pm1/2}}. \tag{22}$$

Thus, (21) can be reformulated to

$$\begin{aligned}
&\frac{(\varphi C_t V)^n}{\Delta t}\left(P_{w,i}^{n+1} - P_{w,i}^{n}\right) \\
&\quad - \left\{T_{tw,i+1/2}\left(P_{w,i+1}^{n+1} - P_{w,i}^{n+1}\right) + T_{tw,i-1/2}\left(P_{w,i-1}^{n+1} - P_{w,i}^{n+1}\right) \right. \\
&\qquad + T_{tw,j+1/2}\left(P_{w,j+1}^{n+1} - P_{w,j}^{n+1}\right) + T_{tw,j-1/2}\left(P_{w,j-1}^{n+1} - P_{w,j}^{n+1}\right) \\
&\qquad \left. + T_{tw,m+1/2}\left(P_{w,m+1}^{n+1} - P_{w,m}^{n+1}\right) + T_{tw,m-1/2}\left(P_{w,m-1}^{n+1} - P_{w,m}^{n+1}\right)\right\} \\
&\quad = V \sum_{k=1}^{Ncv} R_k.
\end{aligned} \tag{23}$$

Equation (23) includes seven pairs of diagonal matrix for the three-dimensional space:

$$\begin{aligned}
&a_{i,j,k}P_{i,j,k-1} + b_{i,j,k}P_{i,j-1,k} + c_{i,j,k}P_{i-1,j,k} + d_{i,j,k}P_{i,j,k} \\
&\quad + e_{i,j,k}P_{i-1,j,k} + f_{i,j,k}P_{i,j+1,k} + g_{i,j,k+1}P_{i,j,k-1} = h_{i,j,k}.
\end{aligned} \tag{24}$$

Based on the UTCHEM simulator (UTCHEM, Version 6.1, 1999), we use the incomplete LU decomposition method to precondition (24) and use the conjugate gradient method to solve (24). In order to improve the accuracy in the front of displacement, we choose the third-order format TVD method [38] as the difference scheme to process the coefficients.

4. Results and Discussion

We use the model to simulate a one-dimensional formation; the parameters are shown in Table 1. The parameters of polar substances are referenced from the experiments [39].

Table 2: Parameters of experimental cores.

Core number	Lengths (mm)	Diameter (mm)	Dry weight (g)	Porosity (%)	Gas-measured permeability ($\times 10^{-3}$ μm^2)
2-1	25.3	39.5	33.3	23.1	2535
2-2	25.1	42.5	35.7	25.7	2513

Table 3: Ion content and salinity of brine.

Ions	Na^+	Ca^+	Mg^{2+}	K^+	Cl^-	HCO_3^-	SO_4^{2-}
Concentration (mg/L)	11.224	768	187	15.0	19.211	7.6	72

Table 4: Displacement experiment data.

Core number	Injected rate (mL/min)	Viscosity (cp)	Interfacial tension (mN/m)	Sweep rate (10^{-5} m/s)	Displacement Efficiency (%)	Residual oil saturation (%)	Capillary number
2-1	1.00	5.3	$1.1E-01$	2.15	65.4	25.5	$1.0E-03$
2-2	1.00	5.3	$2.3E-02$	2.72	74.9	18.8	$6.3E-03$

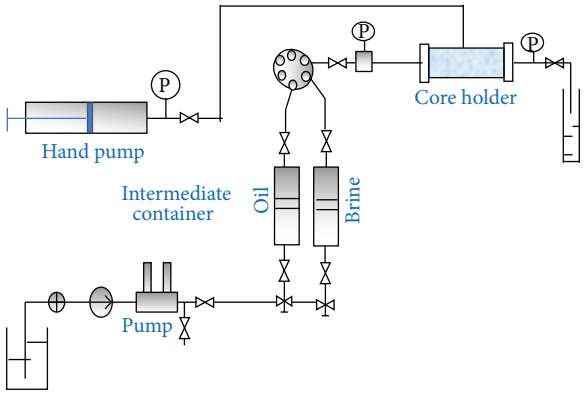

Figure 3: Setups for experimental displacement.

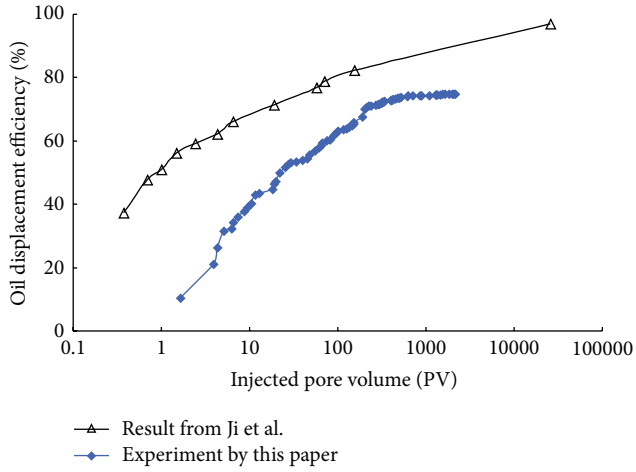

Figure 4: Comparison of the result with experiment by Ji et al. [13]. In Ji's experiment, the core with 2413 mD permeability was from Daqing Oilfield of China and the injected water reached 30,000 PV.

4.1. Experiments and Verification

4.1.1. Experimental Materials and Conditions. The cores used in the experimental material were sealed cores from the reservoir formation (Table 2).

Brine was prepared to simulate the formation water of 1080 mg/L salinity (Table 3). Oil with 5.3 cp of viscosity at 80°C was a mixture of crude oil and light oil.

The temperature was kept at 80°C for all the tests. The brine was injected by a constant-velocity pump of 1.0 mL/min.

4.1.2. Experimental Setup and Procedures. The displacement setup is shown in Figure 3 and the procedures include the following.

(1) The core was saturated with brine and oil, and then core was socked to recover the initial wettability for 15 days.

(2) The relative permeability was determined with 30 PV of brine injected with the nonsteady method, as shown in Figure 5(a), and the pressure and flow rate of oil and water were recorded (Table 4).

(3) After 30 PV of water flooding, 2000 PV of brine was continuously injected and the oil displacement efficiency was also continuously recorded (Figure 4).

(4) The core was saturated with oil again, and then the relative permeability was determined with 30 PV of brine, as shown in Figure 5(b).

4.1.3. Experimental Results and Verification. In order to compare the result with another study, the displacement experiment was compared with results by Ji et al. [13] shown in Figure 4. Due to the different cores in experiments, only trends of increasing of oil displacement efficiency were compared, and the results show that the trends were the same

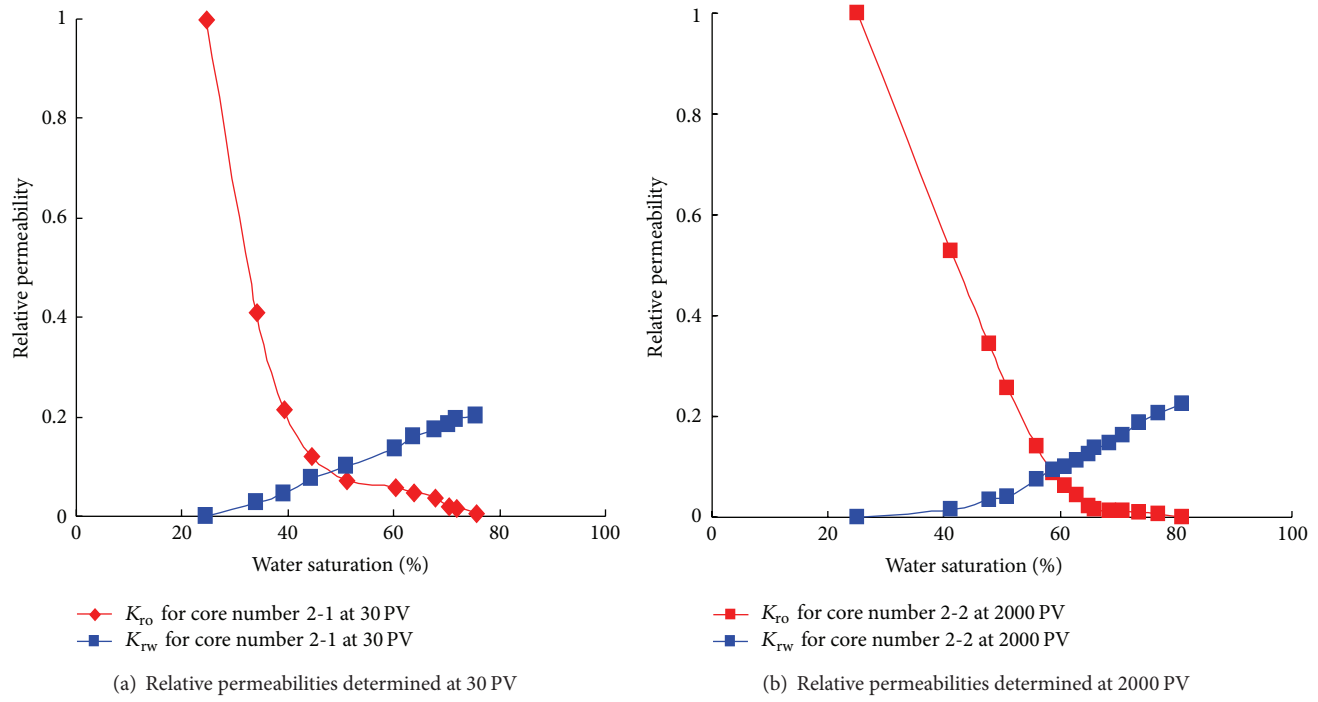

(a) Relative permeabilities determined at 30 PV

(b) Relative permeabilities determined at 2000 PV

FIGURE 5: Relative permeabilities determined at 30 PV and 2000 PV.

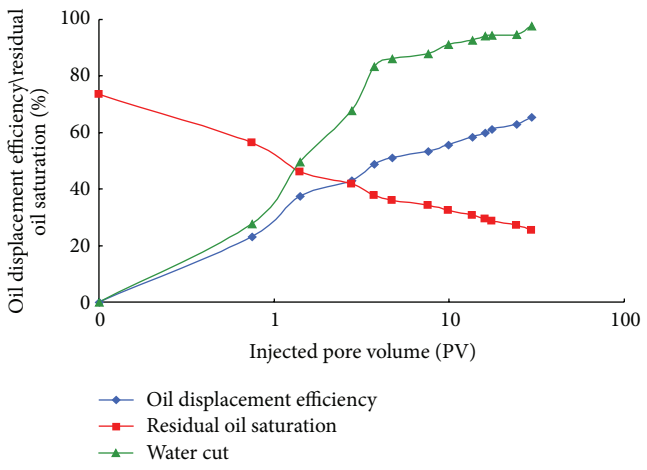

FIGURE 6: Oil displacement efficiency, residual oil saturation, and water cut with semilogarithmic injected pore volume for 30 PV.

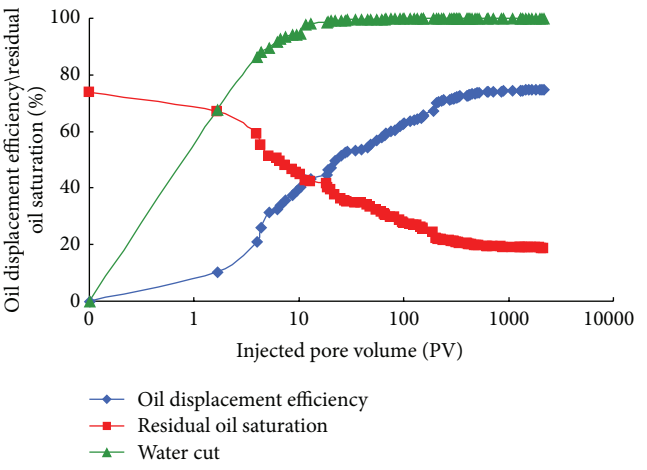

FIGURE 7: Oil displacement efficiency, residual oil saturation, and water cut with injected pore volume for 2000 PV.

for the experiment results of this paper and the results by Ji et al. [13].

The relative permeability curves at C^{max} and C^{min} used in simulation are shown in Figures 5(a) and 5(b), and they represent the conditions with initial wettability and high water-wet wettability. The simulation result shows that the changing trend of oil displacement efficiency (E_d) and residual oil saturation (S_{or}) can match the experimental result well.

In core number 2-1, brine was injected in the pore for 30 PV, the oil displacement was nearly 70%, and residual oil saturation had a value of 25%, shown in Figure 6. From the experiment of core number 2-2, oil displacement efficiency could almost reach 80% while the brine was injected for more than 2000 PV as a high PV, shown in Figure 7. Based on the experiments of core number 2-1 and number 2-2, the oil displacement can be enhanced as the brine injected increases. The water displacement experiment data is shown in Table 4.

Notice that many possible factors can influence the matching result between the simulation and experiment, and a better match can be obtained through adjusting the parameters of adsorption function (9) during the simulation (Figure 8).

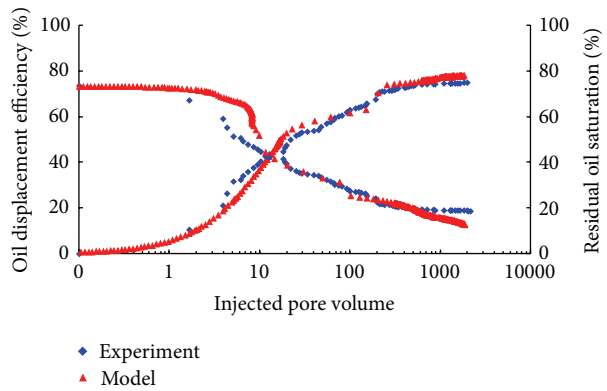

Figure 8: Oil displacement efficiency, residual oil saturation from experiment, and model during long-term water flooding.

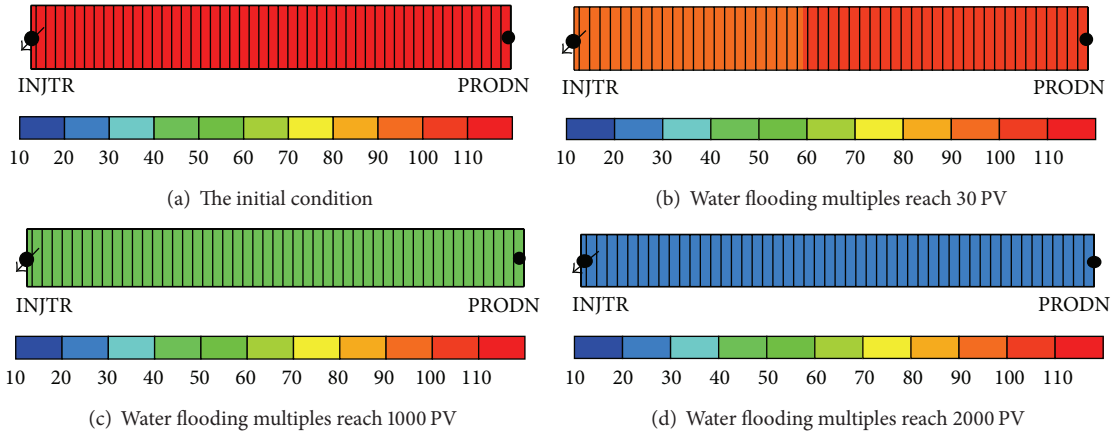

(a) The initial condition (b) Water flooding multiples reach 30 PV

(c) Water flooding multiples reach 1000 PV (d) Water flooding multiples reach 2000 PV

Figure 9: Adsorption contents of clay under the condition of different water flooding multiples (gmole/m^3).

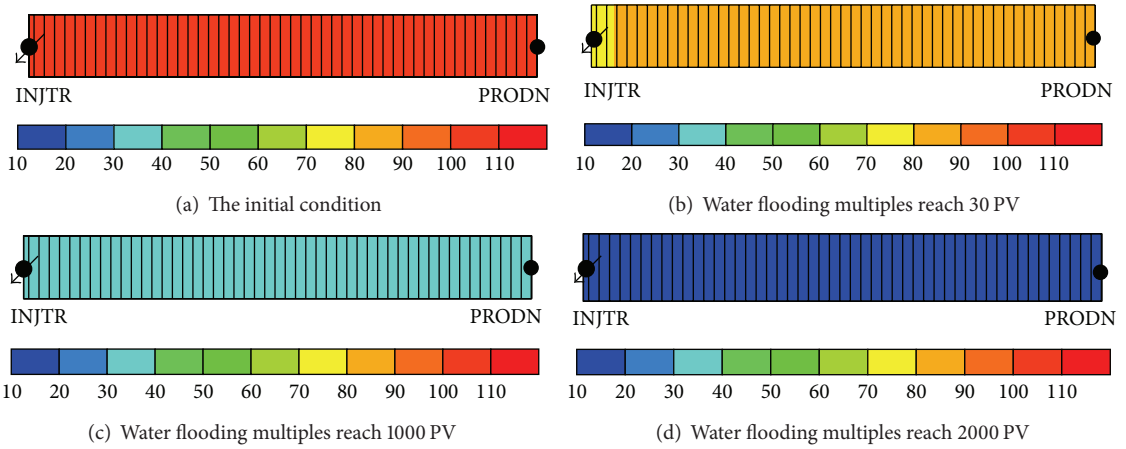

(a) The initial condition (b) Water flooding multiples reach 30 PV

(c) Water flooding multiples reach 1000 PV (d) Water flooding multiples reach 2000 PV

Figure 10: Adsorption contents of AO under the condition of different water flooding multiples (gmole/m^3).

4.2. Change of Polar Substances during Long-Term Water Flooding. The new model can simulate the ion exchange chemical reaction by defining different conditions of ion exchange and clay adsorption properties, and we can obtain the contents of polar substances (C^{AO}_{rock}) and clay on the rock (C^{clay}_{rock}) at different PV of injected brine (Figures 9 and 10). The variations of C^{AO}_{rock} and C^{clay}_{rock} are shown in Figure 11. C^{AO}_{rock} and C^{clay}_{rock} decrease with the increasing PV of injected brine, and the decreasing rate is high between 30 PV and 500 PV during water flooding. When above 500 PV, the C^{AO}_{rock} and C^{clay}_{rock} change slowly, which means that same reduction of polar substances needs more PV of brine injected at the high water

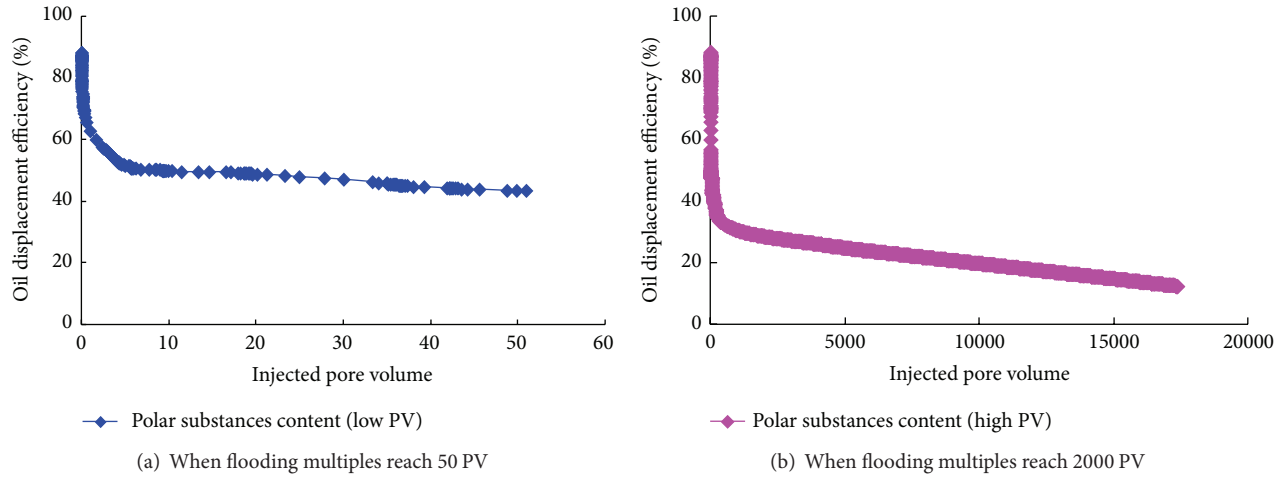

(a) When flooding multiples reach 50 PV

(b) When flooding multiples reach 2000 PV

Figure 11: Oil displacement efficiency under the condition of different water flooding multiples.

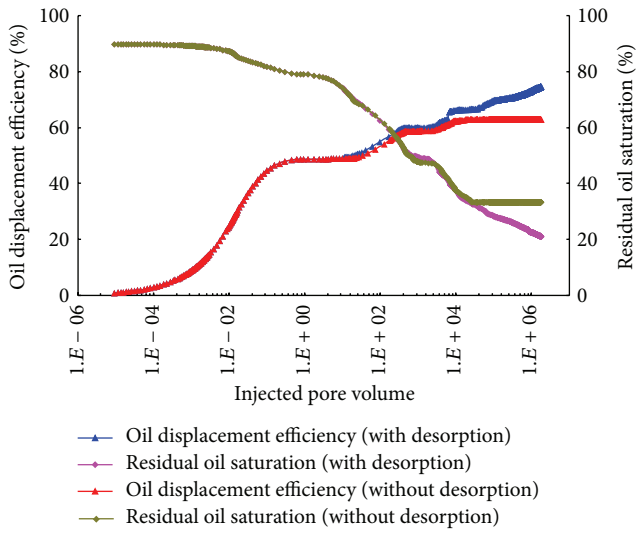

Figure 12: Relationship between water flooding multiples and oil displacement efficiency within different adsorption conditions.

cut stage. This is because the equilibrium of clay adsorption is relatively stable at low water cut, and great washing will break the equilibrium of polar substances adsorbed on clay under high water cut and water saturation above 30 PV.

4.3. Change of Residual Oil Saturation during Long-Term Water Flooding. The polar substances adsorbed on rock surface play an important role in the wettability; the residual oil saturation (S_{or}) could be reduced with the wettability alternating to water-wet. The simulation results for S_{or} and E_d during a long-term water flooding are shown in Figure 12, in which one case considers and the other ignores the desorption of polar substances.

When considering the desorption of polar substances, E_d at low PV (<50 PV) (Figure 11) can reach 60%; during 50–2000 PV E_d continues to increase to 70%, up to 10000 PV, and E_d could reach 75%. Therefore, improving water volume can significantly improve oil displacement efficiency.

Most of conventional reservoir simulators ignore the desorption of polar substances. Here we set K_1 to be equal to 0 (3) to simulate the condition that the desorption is ignored, which implies that the desorption rate $dC_{\text{rock}}^{\text{clay}}/dt$ is equal to zero. The predicted E_d while ignoring the desorption is lower. This is because S_{or} is a constant when the desorption of polar substances is ignored, and only one permeability curve is used in the simulation model. When the desorption of polar substances is taken into account, the wettability alternates to water-wet and the permeability curves under high PV of water injected are used in simulation model. Thus, the gradual reduction of S_{or} during long-term water flooding is reflected in simulation, and the calculated E_d is more accurate.

5. Conclusions

We draw the following conclusions from our study.

(1) The wettability of oil reservoir changes to water-wet during long-term water flooding, and the residual oil saturation gradually reduces and oil displacement efficiency increases. Therefore, the alternation of wettability should be considered during simulation of long-term water flooding; otherwise it will lead to an incorrect history match and unreliable forecasting.

(2) The desorption of polar substances from the rock during long-term water flooding is the mechanism of wettability variation. Since the wettability is reflected by the relative permeability curves in simulation model, the key point to characterize the process of long-term water flooding is to describe the relationship between relative permeability curves and adsorption of polar substances on rock. The factors for wettability variation include polar substances in crude oil, salinity, and pH of brine, clay in rocks, and flow rate during long-term water flooding.

(3) An efficient approach for long-term water flooding simulation is achieved through building a water-oil two-phase multicomponent simulation model. This model describes most important physical phenomena during long-term water flooding, including polar substances desorption, residual oil saturation reduction, and variation of relative permeabilities. The model is solved through an implicit format to process the pressure and through an explicit format to process the coefficients; the third-order format TVD method was selected as the difference scheme to process the coefficients and to improve the accuracy in the front of displacement.

(4) The simulation results have a good match to experimental results. The results have shown that the reduction of polar substances occurs under the condition of high water cut and high water saturation, the residual oil saturation can be gradually reduced by long-term water flooding, and high oil recovery can be obtained by increasing the volume of injected water.

(5) For the field scale, before history match of simulation, a set of configuration parameters should be turned according to one-dimensional experiments, such as ion exchange, clay and polar substances adsorption-desorption, and relative permeability interpolation sets. All these turned parameters could be used in each grid of map brown field for numerical simulation. Then, the polar substances could be calculated for each grid and this value will be used in the relative permeability interpolation process. However, there are some limitations for residual oil reduction in this paper, such as the variation of porosity, and permeability should also be considered. We could define the relation of porosity and permeability with PV number to deal with this variation.

Conflict of Interests

The authors declare that there is no conflict of interests regarding the publication of this paper.

Acknowledgments

The authors gratefully acknowledge that the project was partially funded by the National Natural Science Foundation of China (E040351304220), Beijing Natural Science foundation (no. 3144033), Specialized Research Fund for the Doctoral Program of Higher Education (no. 20130007120014), and Science Foundation of China University of Petroleum, Beijing.

References

[1] P. G. Nutting, *Some Physical and Chemical Properties of Reservoir Rocks Bearing on the Accumulation and Discharge of Oil*, vol. 12, AAPG, 1934.

[2] R. Leach, O. Wagner, H. Wood, and C. Harpke, "A laboratory and field study of wettability adjustment in water flooding," *Journal of Petroleum Technology*, vol. 14, no. 2, pp. 206–212, 2013.

[3] M. O. Denekas, C. C. Mattax, and G. T. Davis, "Effect of crude oil components on rock wettability," *Transactions of the AIME*, vol. 216, p. 330, 1959.

[4] M. M. Kusakov, *Research in Surface Forces*, edited by B. V. Deryagin, Consultants Bureau, New York, NY, USA, 1963.

[5] C. Schmid, "The wettability of petroleum rocks and results of experiments to study effects of variations in wettability of core samples," *Erdoel Kohle*, vol. 17, no. 8, p. 605, 1964.

[6] W. G. Anderson, "Wettability literaure survey—part 1: rock/oil/brine in teractions and the effects of core handling on wettabilty," *Journal of Petroleum Technology*, vol. 38, no. 11, pp. 1125–1144, 1986.

[7] J. S. Buckley, Y. Liu, X. Xie, and N. R. Morrow, "Asphaltenes and crude oil wetting—the effect of oil composition," in *Proceedings of the 10th Symposium on Improved Oil Recovery*, pp. 205–220, April 1996.

[8] L. Cuiec, "Rock/crude-oil interactions and wettability: an attempt to understand their interrelation," in *Proceedings of the SPE Annual Technical Conference and Exhibition*, SPE-13211-MS, Houston, Tex, USA, September 1984.

[9] J. S. Buckley, Y. Liu, and S. Monsterleet, "Mechanisms of wetting alteration by crude oils," *SPE Journal*, vol. 3, no. 1, pp. 54–61, 1998.

[10] R. S. H. Al-Maamari and J. S. Buckley, "Asphaltene precipitation and alteration of wetting: the potential for wettability changes during oil production," *SPE Reservoir Evaluation & Engineering*, vol. 6, no. 4, pp. 210–214, 2003.

[11] A. Graue, B. G. Viksund, and B. A. Baldwin, "Reproducible wettability alteration of low-permeable outcrop chalk," *SPE Reservoir Evaluation & Engineering*, vol. 2, no. 2, pp. 134–140, 1999.

[12] N. R. Morrow, "Physics and thermodynamics of capillary action in porous media," *Journal of Industrial and Engineering Chemistry*, vol. 62, no. 1, pp. 43–50, 1970.

[13] S. Ji, C. Tian, C. Shi, J. Ye, Z. Zhang, and X. Fu, "New understanding on water-oil displacement efficiency in a high water-cut stage," *Petroleum Exploration and Development*, vol. 39, no. 3, pp. 362–370, 2012.

[14] P. P. Jadhunandan and N. R. Morrow, "Effect of wettability on waterflood recovery for crude-oil/brine/rock systems," *SPE Reservoir Engineering*, vol. 10, no. 1, pp. 40–46, 1995.

[15] G. Q. Tang and N. R. Morrow, "Salinity, temperature, oil composition and oil recovery by waterflooding," *SPE Reservoir Engineering*, vol. 12, no. 4, pp. 269–276, 1997.

[16] G.-Q. Tang and N. R. Morrow, "Influence of brine composition and fines migration on crude oil/brine/rock interactions and oil recovery," *Journal of Petroleum Science and Engineering*, vol. 24, no. 2–4, pp. 99–111, 1999.

[17] G. Q. Tang and N. R. Morrow, "Oil recovery by waterflooding and imbibition—invading brine cation valency and salinity," in *Proceedings of the International Symposium of the Society of Core Analysis*, Paper SCA-9911, Golden, Colo, USA, August 1999.

[18] A. Lager, K. J. Webb, I. R. Collins, and D. M. Richmond, "LoSalTM enhanced oil recovery: evidence of enhanced oil recovery at the reservoir scale," in *Proceedings of the SPE/DOE Improved Oil Recovery Symposium*, paper SPE 113976, Tulsa, Okla, USA, April 2008.

[19] A. Lager, K. J. Webb, I. R. Collins, and D. M. Richmond, "LoSalTM enhanced oil recovery: evidence of enhanced oil recovery at the reservoir scale," in *Proceedings of the SPE/DOE Improved Oil Recovery Symposium*, Paper SPE 113976, Tulsa, Okla, USA, April 2008.

[20] P. Vledder, J. C. Fonseca, T. Wells, I. Gonzalez, and D. Ligthelm, "Low salinity water flooding: proof of wettability alteration on a field wide scale," in *Proceedings of the SPE Improved Oil Recovery Symposium*, Paper SPE 129564, pp. 200–209, Tulsa, Okla, USA, April 2010.

[21] K. J. Webb, C. J. J. Black, and Al-Ajeel, "Low salinity oil recovery-log-inject-log," in *Proceedings of the SPE/DOE Symposium on Improved Oil Recovery*, Paper SPE 89379, Tulsa, Okla, USA, April 2004.

[22] K. J. Webb, C. J. J. Black, and I. J. Edmonds, "Low salinity oil recovery: the role of reservoir condition corefloods," in *Proceedings of the 13th EAGE Symposium on Improved Oil Recovery*, Paper C18, Budapest, Hungary, April 2005.

[23] K. J. Webb, A. Lager, and C. J. Black, "Comparison of high/low salinity water/oil relative permeability," in *Proceedings of the International Symposium of the Society of Core Analysts*, Abu Dhabi, UAE, October–November 2008.

[24] S. M. Rivet, *Coreflooding oil displacements with low salinity brine [M.S. thesis]*, University of Texas at Austin, 2009.

[25] I. Fjelde, S. V. Asen, and A. Omekeh, "Low salinity water flooding experiments and interpretation by simulations," in *Proceedings of the 18th SPE Improved Oil Recovery Symposium*, Paper SPE 154142, Tulsa, Okla, USA, April 2012.

[26] J. Zhang, W. Yan, and Q. Liu, "Field practice of production with very high water cut under water flooding," *Petroleum Exploration and Development*, vol. 13, no. 1, pp. 50–54, 1986.

[27] Y. S. Wu and B. Bai, "Efficient simulation for low salinity water-flooding in porous and fractured reservoirs," in *Proceedings of the SPE Reservoir Simulation Symposium*, SPE-118830-MS, The Woodlands, Tex, USA, February 2009.

[28] C. T. Q. Dang, L. X. Nghiem, Z. J. Chen, and Q. P. Nguyen, "Modeling low salinity waterflooding: ion exchange, geochemistry and wettability alteration," in *Proceedings of the SPE Annual Technical Conference and Exhibition*, SPE-166447-MS, New Orleans, La, USA, September–October 2013.

[29] A. V. Ryazanov, K. S. Sorbie, and M. I. J. van Dijke, "Structure of residual oil as a function of wettability using pore-network modelling," *Advances in Water Resources*, vol. 63, pp. 11–21, 2014.

[30] S. T. Taqvi, A. Almansoori, and G. Bassioni, "Modeling the impact of wettability alterations on calcium carbonate system for crude oil and asphaltenic solutions," *Industrial & Engineering Chemistry Research*, vol. 53, no. 12, pp. 4773–4777, 2014.

[31] A. Skauge, S. Standal, S. O. Boe, and A. M. Blokhus, "Effects of organic acids and bases, and oil composition on wettability," in *Proceedings of the SPE Annual Technical Conference*, 1999.

[32] C. E. Brown and E. L. Neustadter, "The wettability of oil/water/silica systems with reference to oil recovery," *Journal of Canadian Petroleum Technology*, vol. 19, no. 3, pp. 100–110, 1980.

[33] P. Zhang, M. T. Tweheyo, and T. Austad, "Wettability alteration and improved oil recovery by spontaneous imbibition of seawater into chalk: impact of the potential determining ions Ca^{2+}, Mg^{2+}, and SO_4^{2-}," *Colloids and Surfaces A: Physicochemical and Engineering Aspects*, vol. 301, no. 1–3, pp. 199–208, 2007.

[34] C. Maschio, A. C. Vidal, and D. J. Schiozer, "A framework to integrate history matching and geostatistical modeling using genetic algorithm and direct search methods," *Journal of Petroleum Science and Engineering*, vol. 63, no. 1–4, pp. 34–42, 2008.

[35] M. K. Zahoor and M. N. Derahman, "New approach for improved history matching while incorporating wettability variations in a sandstone reservoir—Field implementation," *Journal of Petroleum Science and Engineering*, vol. 104, pp. 27–37, 2013.

[36] M. Delshad, G. A. Pope, and K. Sepehrnoori, "A compositional simulator for modeling surfactant enhanced aquifer remediation, 1 Formulation," *Journal of Contaminant Hydrology*, vol. 23, no. 4, pp. 303–327, 1996.

[37] M. Delshad, G. A. Pope, and L. W. Lake, "Two-and three-phase relative permeabilities of micellar fluids," *SPE Formation Evaluation*, vol. 2, no. 3, pp. 327–337, 1987.

[38] J. Liu, M. Delshad, G. A. Pope, and K. Sepehrnoori, "Application of higher-order flux-limited methods in compositional simulation," *Transport in Porous Media*, vol. 16, no. 1, pp. 1–29, 1994.

[39] H. J. Hill, "Cation exchange in chemical flooding: part 3—experimental," *Society of Petroleum Engineers Journal*, vol. 18, no. 6, pp. 445–456, 1978.